FULL PAPER

Dalton
www.rsc.org/dalton

The structural and electrochemical properties of new bis-imido transition metal salen complexes

Majid Motevalli,[a] A. Duro Oduwole,[a] Bernardetta C. Parkin,[a] Ramkrishna Ramnauth,[a] Alice C. Sullivan[a] and Nikolas Kaltsoyannis[b]

[a] *Department of Chemistry, Queen Mary, University of London, Mile End Road, UK E1 4NS. E-mail: a.c.sullivan@qmul.ac.uk*

[b] *Department of Chemistry, University College London, 20 Gordon Street, UK WC1H 0AJ. E-mail: uccanka@ucl.ac.uk*

Received 28th April 2003, Accepted 15th July 2003
First published as an Advance Article on the web 5th August 2003

The reaction between $[M(N^tBu)_2(NH^tBu)_2]$ (M = Mo or W) and dianionic N_2O_2 coordinating salen ligands afforded new bis-imido salen Mo(VI) and W(VI) transition metal complexes $[W(N^tBu)_2\{(3,5\text{-}^tBu_2)_2salen\}]$ **1**, $[W(N^tBu)_2\{(3\text{-}MeO)_2salen\}]$ **2**, $[W(N^tBu)_2\{(4\text{-}MeO)_2salen\}]$ **3**, $[W(N^tBu)_2\{(5\text{-}MeO)_2salen\}]$ **4**, $[W(N^tBu)_2(salen)]$ **5**, $[Mo(N^tBu)_2\{(3,5\text{-}^tBu_2)_2salen\}]$ **6**, $[Mo(N^tBu)_2\{(4\text{-}MeO)_2salen\}]$ **7** and $[Mo(N^tBu)_2(salen)]$ **8**. Compounds **1**–**8** were characterised by NMR, IR and FAB mass spectrometry while compound **6** was additionally characterised by X-ray crystallography. Both the Mo and W series adopt structures having the Schiff bases in the strained β-*cis* configuration and the structural parameters suggest that this is dictated by steric rather than electronic factors while the *cis* configuration of the imido groups results from expected electronic preferences. The redox chemistry of all these compounds has been studied by cyclic voltammetry and additionally by chemical routes and controlled current electrolytic routes in the case of **1**. EPR and density function calculations on oxidised **1** confirmed that the oxidation process is imido centred.

Introduction

Transition metal imido complexes attract great interest in view of the beneficial π-donor properties of the imido group and their application in a growing number of catalytic processes particularly homogeneous polymerisation and imine metathesis.[1] In a recent communication we reported on the first examples of bis-imido transition metal Schiff-base complexes of the type $[W(N^tBu)_2L]$, where L = $(3,5\text{-}^tBu_2)_2$salen **1** or other related substituted salen ligands.[2] Well documented arguments allowed us to conclude that the formation of the non-planar salen arrangement (see Fig. 1) in compound **1** was driven by the electronic benefits associated with the mutually bis-*cis*-imido relationship.[3] We also reported that compound **1** readily undergoes a low energy reversible one-electron oxidation process.[2]

In this paper we report on the extension of our synthetic and structural studies to analogous molybdenum compounds and give the detailed results of electrochemical studies on these complexes. We report further on our analysis of the low energy oxidation product of compound **1**, analysed with the aid of EPR spectroscopy and density function calculations.

Synthesis and structural chemistry

The bis-imido salen complexes $[M(N^tBu)_2L]$ **1**–**8** were prepared by the alcoholysis reaction of $[M(N^tBu)_2(NH^tBu)_2]$ (M = Mo or W) in toluene using the diprotonated Schiff-bases LH_2 as illustrated in Scheme 1. Some details on characterisation are included in Table 1.

Solution phase ^{1}H NMR spectroscopic data of the bis-imido complexes clearly indicates the folded asymmetric β-*cis* arrangement of the salen ligands (Table 2 and Fig. 2).

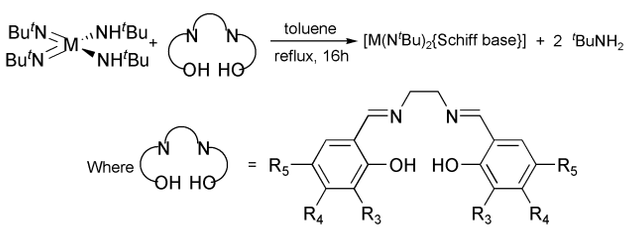

Scheme 1

All spectra contain two imine resonances (upfield of free base) rather than a single resonance as found for symmetrical planar or α-*cis* Schiff base geometries.[4,5] The folded nature of the ligand is most strikingly reflected in the appearance of four multiplets due to the two methylene groups of the ethylenediimine backbone which display an AA′BB′ pattern. A singlet is observed for these methylene protons in the free Schiff base and in planar complexes. The IR spectra of the compounds also indicate the twisted nature of the salen ligand with two C=N bands being observed while only one is found for planar and α-*cis* Schiff base geometries[4,5] (see Table 1).

The molecular structure of $[Mo(N^tBu)_2\{(3,5\text{-}^tBu_2)_2salen\}]$ **6**, was determined by single crystal X-ray crystallography and is shown in Fig. 3.

$[Mo(N^tBu)_2\{(3,5\text{-}^tBu_2)_2salen\}]$ is isostructural with the previously reported tungsten analogue, $[W(N^tBu)_2\{(3,5\text{-}^tBu_2)_2salen\}]$ **1**. Some selected bond lengths and angles are given in Table 3 and depict the distorted octahedral geometry at the molybdenum centre.

Angles subtended by mutually *cis*-ligating groups are in the range 70.93(8)–106.8(9)°. As found for **1**, *trans* influence likely

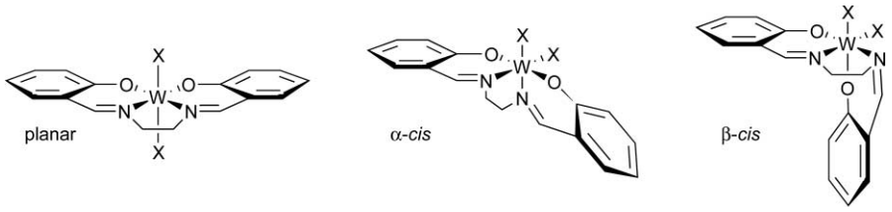

Fig. 1 Possible geometries adopted by metal salen octahedral complexes, $[MLX_2]$.

DOI: 10.1039/b304627c

Table 1 Selected analytical data for the bis-imido salen compounds **1**–**8**

Compound	Colour	Yield (%)	Elemental analysis[a] (%)			FAB-MS (M^+) (*m*/*z*)	ν(C=N)/cm^{-1}
			C	H	N		
[W(N^{t}Bu)$_2${(3,5-^{t}Bu$_2$)$_2$salen}] (**1**)	Red	99	58.54 (58.82)	7.85 (7.90)	6.95 (6.86)	817.4615	1640, 1628
[W(N^{t}Bu)$_2${(3-MeO)$_2$salen}] (**2**)	Yellow	75	48.01 (47.86)	5.50 (5.56)	8.37 (8.59)	653.2329	1642, 1602
[W(N^{t}Bu)$_2${(4-MeO)$_2$salen}] (**3**)	Orange	96	47.55 (47.86)	5.43 (5.56)	8.41 (8.59)	653.2320	1635, 1594
[W(N^{t}Bu)$_2${(5-MeO)$_2$salen}] (**4**)	Yellow	51	48.33 (47.86)	5.54 (5.56)	8.31 (8.59)	653.2317	1645, 1615
[W(N^{t}Bu)$_2$(salen)] (**5**)	Yellow	37	48.51 (48.66)	5.32 (5.44)	9.64 (9.46)	593.2122	1646, 1616
[Mo(N^{t}Bu)$_2${(3,5-^{t}Bu$_2$)$_2$salen}] (**6**)	Red–orange	94	65.78 (65.91)	8.81 (8.85)	7.52 (7.69)	731.4160	1640, 1611
[Mo(N^{t}Bu)$_2${(4-MeO)$_2$salen}] (**7**)	Orange	96	55.14 (55.32)	6.38 (6.43)	9.87 (9.92)	566.1777	1625, 1601
[Mo(N^{t}Bu)$_2$(salen)] (**8**)	Yellow	45	56.97 (57.14)	6.21 (6.39)	10.89 (11.11)	506.1595	1655, 1617

[a] Required values in parentheses.

Table 2 ^{1}H NMR data for the bis-imido salen compounds **1**–**8**

Compound	Imine protons	Aromatics protons	Methylene protons	Substituents on salen	Imido protons
[W(N^{t}Bu)$_2${(3,5-^{t}Bu$_2$)$_2$salen}] (**1**)	8.2 (s, 1H) 8.1 (s, 1H)	7.5 (d, 2H) 7.4 (d, 2H) 7.1 (d, 2H) 7.0 (d, 2H)	4.5 (m, 1H) 4.1 (m, 1H) 4.0 (m, 1H) 3.4 (m, 1H)	1.4 (s, 9H) 1.4 (s, 9H) 1.3 (s, 9H) 1.3 (s, 9H)	1.1 (s, 9H) 0.9 (s, 9H)
[W(N^{t}Bu)$_2${(3-MeO)$_2$salen}] (**2**)	8.25 (s, 1H) 8.10 (s, 1H)	7.1 (d, 1H) 6.95 (m, 3H) 6.7 (t, 1H) 6.5 (t, 1H)	4.5 (m, 1H) 4.2(m, 1H), 4.0 (m, 1H) 3.5 (m, 1H)	4.0 (s,3H) 4.0 (s, 3H),	1.06 (s, 9H) 0.94 (s, 9H)
[W(N^{t}Bu)$_2${(4-MeO)$_2$salen}] (**3**)	8.1 (s, 1H) 8.0 (s, 1H)	7.1 (m, 2H) 6.7 (d, 1H) 6.5 (d, 1H) 6.4 (m, 1H) 6.3 (m, 1H)	4.4 (s, 1H) 4.2 (s, 1H) 3.9 (s, 1H) 3.5 (s, 1H)	3.8 (s, 3H) 3.8 (s, 3H)	1.1 (s, 9H) 1.0 (s, 9H)
[W(N^{t}Bu)$_2${(5-MeO)$_2$salen}] (**4**)	8.5 (s, 1H) 8.4 (s, 1H)	7.4 (m, 3H) 7.3 (d, 1H) 7.0 (m, 1H)	4.8 (m, 1H) 4.5 (m, 1H) 4.3 (m, 1H) 3.8 (m, 1H)	4.1 (s, 3H) 4.0 (s, 3H)	1.3 (s, 9H) 1.3 (s, 9H)
[W(N^{t}Bu)$_2$(salen)] (**5**)	8.27 (s, 1H) 8.14 (s, 1H)	7.4 (m, 3H) 7.3 (m, 2H) 7.1 (m, 1H) 7.0 (m, 1H) 6.8 (m, 1H) 6.6 (m, 1H)	4.46 (m, 1H) 4.23 (m, 1H) 4.01 (m, 1H) 3.53 (m, 1H)		1.04 (s, 9H) 0.96 (s, 9H)
[Mo(N^{t}Bu)$_2${(3,5-^{t}Bu$_2$)$_2$salen}] (**6**)	8.2 (s, 1H) 8.2 (s, 1H)	7.5 (d, 2H) 7.4 (d, 2H) 7.1 (d, 2H) 7.0 (d, 2H)	4.3 (m, 1H) 3.9 (m, 2H) 3.4 (m, 1H)	1.5 (s, 9H) 1.4 (s, 9H) 1.3 (s, 9H) 1.3 (s, 9H)	1.1 (s, 9H) 0.9 (s, 9H)
[Mo(N^{t}Bu)$_2${(4-MeO)$_2$salen}] (**7**)	7.5 (s, 1H) 7.4 (s, 1H)	7.1 (m, 3H) 6.7 (d, 1H) 6.5 (d, 2H)	3.8 (s, 1H) 3.1 (s, 1H) 2.8 (s, 1H)	3.2 (s, 3H) 3.2 (s, 3H)	1.3 (s, 9H) 1.2 (s, 9H)
[Mo(N^{t}Bu)$_2$(salen)] (**8**)	8.34 (s, 1H) 8.19 (s, 1H)	7.3 (m, 4H) 7.1 (m, 2H 6.8 (t, 1H) 6.6 (t, 1H)	4.46 (m, 1H) 4.00 (m, 2H) 4.01 (m, 1H)		1.04 (s, 9H) 0.96 (s, 9H)

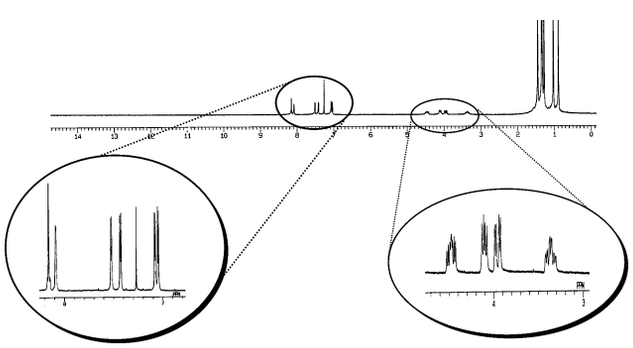

Fig. 2 ^{1}H NMR of [W(N^{t}Bu)$_2${(3,5-^{t}Bu$_2$)$_2$salen}]**1** showing the common features of the β-*cis* salen coordination.

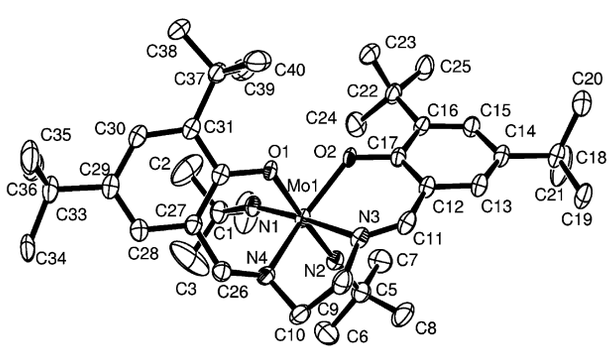

Fig. 3 Crystal structure of [Mo(N^{t}Bu)$_2${(3,5-^{t}Bu$_2$)$_2$salen}]**6**.

underpins the difference between the two molybdenum–oxygen bond distances 2.0012(17) Å (*trans*-imine), 2.1220(17) Å (*trans*-imido) and the two molybdenum–nitrogen bond distances 2.157(2) Å (*trans* phenoxy), 2.249(2) Å (*trans*-imido). The imido bond distances are essentially identical: Mo(1)–N(1) 1.682(2), Mo(1)–N(2) 1.686(2) and amongst the shortest found for molybdenum imido systems. However as for **1**, the imido group *trans* to the imine nitrogen is more acute, C(1)–N(1)–Mo(1), 159.6(2)°, than the imido *trans* to the phenoxy group, C(5)–

Table 3 Selected bond lengths (Å) and angles (°) for compound **6**

Mo(1)–N(1)	1.682(2)	Mo(1)–O(1)	2.1220(17)
Mo(1)–N(2)	1.686(2)	Mo(1)–N(4)	2.157(2)
Mo(1)–O(2)	2.0012(17)	Mo(1)–N(3)	2.249(2)
C(1)–N(1)–Mo(1)	159.6(2)	N(2)–Mo(1)–N(4)	96.72(9)
C(5)–N(2)–Mo(1)	177.5(2)	O(2)–Mo(1)–N(4)	147.15(8)
N(1)–Mo(1)–N(2)	100.66(10)	O(1)–Mo(1)–N(4)	76.43(7)
N(1)–Mo(1)–O(2)	106.08(9)	N(1)–Mo(1)–N(3)	167.84(9)
N(2)–Mo(1)–O(2)	99.33(9)	N(2)–Mo(1)–N(3)	87.30(9)
N(1)–Mo(1)–O(1)	91.94(9)	O(2)–Mo(1)–N(3)	81.38(7)
N(2)–Mo(1)–O(1)	166.52(8)	O(1)–Mo(1)–N(3)	79.50(7)
O(2)–Mo(1)–O(1)	81.55(7)	N(4)–Mo(1)–N(3)	70.93(8)
N(1)–Mo(1)–N(4)	98.79(9)		

N(2)–Mo(1), 177.5(2)°. This may reflect the comparative *trans*-influence of these two groups but is more likely attributable to the different steric interactions between the imido groups and the nearest Schiff base aryl fragments.

It is interesting that the strained Schiff base conformation, β-*cis*, is adopted in these complexes. This would appear to be driven entirely by electronic preferences and the avoidance of alternative competitive *trans* relationships between the imido groups. A planar arrangement would result in the most competitive situation with imido groups *trans* to one another. An α-*cis* arrangement would not be expected because of the strain associated with the ethylenediimine chelating fragment in this conformation.

Electrochemistry

Cyclic voltammetry. The redox behaviour of compounds **1**–**7** was examined by cyclic voltammetry. The experiments were carried out in a number of solvents including, THF, DMF, CH_3CN, DCM and DMSO containing 0.1 M $^n Bu_4NPF_6$ as the supporting electrolyte. The observed redox processes were examined at a range of scan rates from 0.1 to 5 V s^{-1}. Compounds **1**–**7** readily undergo one-electron oxidation and reduction processes (Fig. 4). The results are summarised in Table 4.

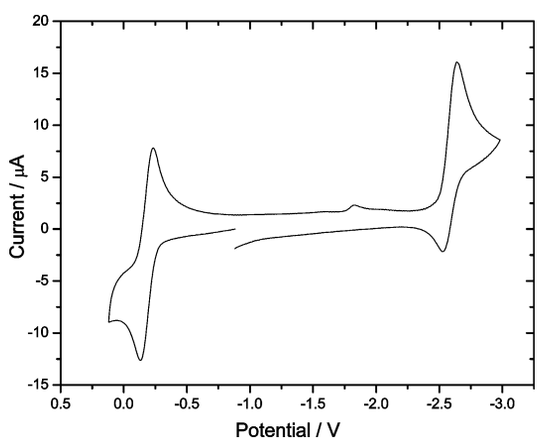

Fig. 4 Cyclic voltammogram of the oxidation process of [W(N^{t}Bu)$_2${(3,5-^{t}Bu$_2$)$_2$salen}]**1** in DMF containing 0.1 M $^n Bu_4NPF_6$, sweep-rate 1 V s^{-1}.

A ligand centred low energy one-electron oxidation process is observed for all the compounds. The phenyl ring substituents in the salen ligands can be considered to affect the donor properties relative to unsubstituted salen but we failed to observe any differentiation between the Schiff bases used in this work. Although an analogue of **1** with electron withdrawing nitro groups in place of the tertiary butyls was prepared in the course of this work, its electrochemistry could not be studied owing to poor solubility. The reversibility of the oxidation process is apparently solvent dependent. However it is noteworthy that the process is reversible in DMSO for compounds **1**, **3** and **4** and quasi-reversible for **2**. Oxidation of **2** is even more markedly quasi-reversible in THF as illustrated by the cyclic voltammogram shown in Fig. 5. Overall however, the relative stability of the radical cations in this series does not appear to be markedly influenced by these Schiff-base substituents.

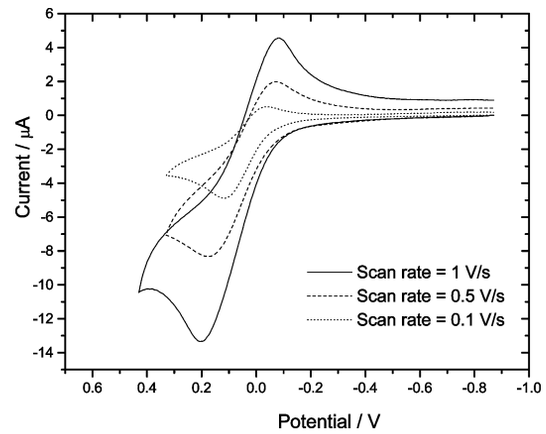

Fig. 5 Cyclic voltammogram of the oxidation process of [W(N^{t}Bu)$_2${(3-MeO)$_2$salen}]**2** in THF containing 0.1 M $^n Bu_4NPF_6$ at sweep-rates of 0.1, 0.5 and 1 V s^{-1}.

One-electron quasi-reversible reduction was observed for compounds **1** and **6**. Irreversible reduction was observed in the other cases. The EPR spectrum of the chemically reduced **1** (Na/Hg one equivalent in THF) was consistent with a metal centred radical (g_{av} = 1.998). Others have suggested similar reduction processes are metal centred.[6] We note that Leung *et al*. have observed metal based reduction at −0.74 V (reversible) for [Cr(N^{t}Bu)$_2$(terpy)](BF$_4$)$_2$], −1.2 V (reversible) for [Cr(N^{t}Bu)$_2$(OAr)$_2$] and *ca.* −2.0 V (irreversible) for [Cr(N^{t}Bu)$_2$Cl$_2$], all in acetonitrile.[7] However it should be noted that density function calculations on **1** predict the LUMO and the LUMO+1 (−2.96 and −2.81 eV) to be salen based N–C pπ* and C–O pπ*. The LUMO+2 orbital, −1.49 eV, has d-character, being W–N (dπ–pπ)* where the imido N is *trans* to the phenoxy group.

Detailed studies on radical cation 1^+. The observation of a low energy reversible oxidation process for several of the compounds warranted further investigation. Compound **1** with $E_{1/2}$ at −0.01 V *vs.* $Cp_2Fe^{0/+}$ was selected for this purpose. In comparison with the series **1**–**7**, other bis-imido compounds we have examined show more complex oxidation behaviour. For example, we observed irreversible oxidation for the pseudo-tetrahedral [W(N^{t}Bu)$_2$(NH^{t}Bu)$_2$] and at least three overlapping reversible oxidation processes for the pseudo-octahedral bis-imido complex [Mo(N^{t}Bu)$_2$Cl$_2$(dme)] (dme = dimethoxyethane) with half-wave potentials in the region 1.21–1.66 V *vs.* $Cp_2Fe^{0/+}$ in CH_3CN. For the free Schiff-base, an irreversible oxidation at 1.34 V *vs.* $Cp_2Fe^{0/+}$ in CH_3CN was observed. We are not aware of cyclic voltammetry studies on other simple six-coordinated Group 6 transition metal compounds of the type [(RN)$_2$-MX$_2$L′$_2$] but our observations suggested that the radical cations from **1**–**7** were unusually stable. In order to study the radical cations further by EPR we needed to use preparative methods to generate them.

This was achieved using chemical oxidation of **1** ($AgPF_6$ one equivalent in THF) as well as controlled current electrolytic oxidation of **1**. Products from both routes were examined by EPR spectroscopy. Identical spectra for oxidised products from both methods were recorded at 298 K showing a quintet (g_{av} = 2.015, a = 10.93 G) consistent with a radical coupled to two equivalent nitrogens (Fig. 6).

Spectra of chemically oxidised **1** were recorded in the temperature range 140–310 K. The spectrum was unchanged at

Table 4 Electrochemical data of metal imido complexes **1**–**7** [All data reported at sweep-rate = 1 V s^{-1}, peak–peak separations for reversible (r) and quasi-reversible (q) processes (mV) are in parentheses, where appropriate, (i) denotes an irreversible process. All potentials are in V *vs.* the ferrocene–ferrocenium ($Cp_2Fe^{0/+}$) couple.]

Compound	Solvent	Oxidation	Reduction
$[W(N^tBu)_2\{(3,5\text{-}^tBu_2)_2salen\}]$ (**1**)	THF	−0.08 (q) (245)	−2.71 V (q) (330)
$[W(N^tBu)_2\{(3,5\text{-}^tBu_2)_2salen\}]$ (**1**)	DCM	−0.13 V (q) (220)	–
$[W(N^tBu)_2\{(3,5\text{-}^tBu_2)_2salen\}]$ (**1**)	DMF	0.18 (r) (100)	−2.59 (q) (110)
$[W(N^tBu)_2\{(3,5\text{-}^tBu_2)_2salen\}]$ (**1**)	CH_3CN	0.00 (r) (90)	–
$[W(N^tBu)_2\{(3,5\text{-}^tBu_2)_2salen\}]$ (**1**)	DMSO	0.03 (r) (56)	−2.37 (q) (235)
$[W(N^tBu)_2\{(3\text{-}MeO)_2salen\}]$ (**2**)	DMSO	0.06 (q) (130)	−2.32 (i)
$[W(N^tBu)_2\{(3\text{-}MeO)_2salen\}]$ (**2**)	THF	0.06 (q) (285)	−2.54 (i)
$[W(N^tBu)_2\{(4\text{-}MeO)_2salen\}]$ (**3**)	DMSO	0.20 (r) (100)	−2.24 (i)
$[W(N^tBu)_2\{(4\text{-}MeO)_2salen\}]$ (**4**)	THF	−0.05 (q) (145)	−2.72 (i)
$[W(N^tBu)_2\{(5\text{-}MeO)_2salen\}]$ (**4**)	DMSO	0.12 (r) (90)	−2.19 (i)
$[W(N^tBu)_2\{(5\text{-}MeO)_2salen\}]$ (**4**)	THF	−0.02 (q) (210)	−2.62 (i)
$[W(N^tBu)_2(salen)]$ (**5**)	THF	−0.08 (q) (355)	−2.63 (i)
$[Mo(N^tBu)_2\{(3,5\text{-}^tBu_2)_2salen\}]$ (**6**)	THF	0.20 (q) (300)	−2.44 (q) (180)
$[Mo(N^tBu)_2\{(4\text{-}MeO)_2salen\}]$ (**7**)	THF	−0.16 (q) (395)	−2.85 (i)

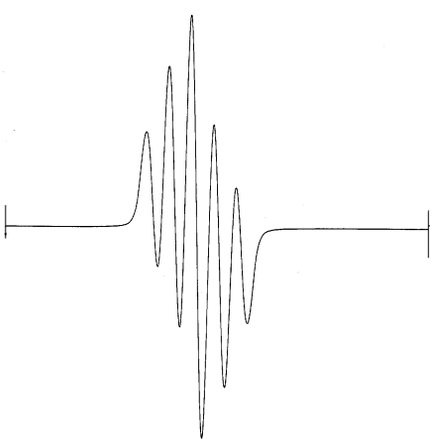

Fig. 6 EPR spectrum of oxidised compound $[W(N^tBu)_2\{(3,5\text{-}^tBu_2)_2\text{-}salen\}]$**1** at 298 K ($g_{av}$ = 2.015, a = 10.93 G).

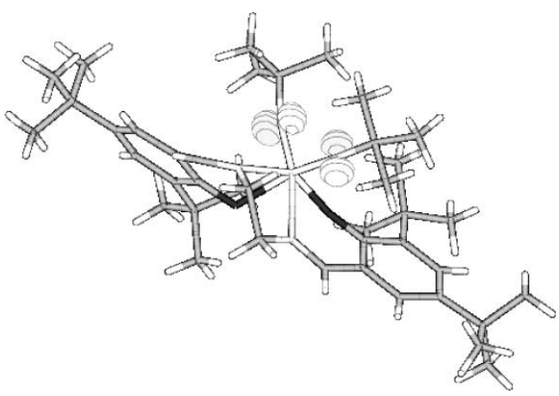

Fig. 7 Three-dimensional representation of the HOMO of **1**, generated from the ADF TAPE21 (binary output) file using the ADFrom99 and MOLDEN programs[27] and using a MOLDEN 'space' value of 0.1 (for details of both MOLDEN and ADFrom99, the reader is directed to http://www.caos.kun.nl/~schaft/molden/molden.html).

200 K, but anisotropic broadening of the quintet was seen at temperatures below 200 K. There was no evidence of satellites to indicate coupling to the tungsten metal centre (^{183}W, I = 1/2, 14.3%). A broad range of spectral widths up to 6000 G and a wide temperature range (140–310 K) was investigated. By contrast, Srinivasen and Kochi reported the EPR spectrum of the chromium Schiff-base complex $[CrO(Me_4salen)]^+$, which clearly shows a radical delocalised over the Schiff-base nitrogens and the chromium metal centre, with satellites indicating coupling to chromium (^{53}Cr, I = 3/2, 9.50%), *i.e.* a central quintet and four quintet satellites were seen.[8] In another report a reversible couple at 0.9 V was assigned to Schiff base ligand centred oxidation in the compound $[Cr(\{(3,5\text{-}^tBu_2)_2salen\})(N^tBu)]BF_4$.[9]

The EPR spectrum of $\mathbf{1}^+$ cannot be explained in terms of a radical localised on the substituted salen ligand as further coupling to protons in the ethylene bridge would have been observed. It therefore appears that the EPR spectrum arises from the unpaired electron coupling to the two imido nitrogen atoms. Interestingly, the absence of tungsten satellites indicates that coupling is not directly mediated by the metal centre.

In order to probe these assertions further, density functional theory calculations on **1** were performed, taking the previously determined[2] crystallographic coordinates as structural input. These calculations fully support our experimental conclusions, as the HOMO of **1** is found to be primarily localised (*ca.* 75%, Mulliken analysis) on the imido nitrogen atoms, with an approximately equal contribution from both nitrogens. In addition, and in-keeping with the EPR spectra, negligible metal character (<2%) is found in this orbital, and only a very minor contribution from the oxygen and nitrogen atoms of the salen ligands. A three-dimensional representation of the HOMO of **1** is shown in Fig. 7; this orbital is clearly an out-of-phase combination of imido nitrogen p-functions.

We have also calculated the electronic structure of $\mathbf{1}^+$, at the geometry of **1**, and find that the half-filled orbital retains the essential features of **1**, *i.e.* it is also primarily localised on the imido nitrogen atoms. While many theroetical studies of imido complexes have been reported, the study by Schrock and co-workers on the formally 20e complex $[Os(NAr)_3]$ (Ar = 2,6-C_6H_3-*i*-Pr_2) is relevant in the present context.[10] The presence of an occupied imido-ligand-centred non-bonding orbital (HOMO−1) was deemed to prevent electronic supersaturation at the metal centre in $[Os(NAr)_3]$. The HOMO in $[Os(NAr)_3]$ has high d-character and, to our knowledge, this is the case in many imido complexes. The imido-centred non-bonding orbital in **1** undoubtedly performs a role in preventing electronic supersaturation at tungsten but the situation is different from $[Os(NAr)_3]$ in that the non-bonding orbital is the HOMO in this case and the oxidation chemistry of the complex is thus imido-ligand centred. While the electrochemistry of $[Os(NAr)_3]$ compounds was not reported, reversible couples observed in some previous redox studies on imido complexes have been attributed to imido centred oxidation. McCleverty and Ward proposed that the redox couple in Mo(VI) complexes $[Mo(O)(Tp^{Me,Me})Cl(NR)]$ (R = $C_6H_4NMe_2$-4, $C_6H_4NH_2$-4) and $[\{Cl(O)(Tp^{Me,Me})Mo\}_2(NC_6H_4N)]$ were likely due to imido oxidation.[11] Che and co-workers reported that the series $[M(Me_3\text{-}tacn)(N^tBu)_2Cl]X$ (X = Cl, ClO_4, M = Cr(VI), Mo(VI)) displayed quasi-reversible redox couples in the range +0.86–1.20 V *vs.* $Cp_2Fe^{0/+}$ and they also proposed imido-centred oxidation.[6] Wilkinson and co-workers reported that solutions from Ag^+ oxidation of $[Mn(N^tBu)_2(\mu\text{-}N^tBu)]_2$ displayed an EPR triplet

associated with a single imido-nitrogen centred radical.[12] As far as we are aware, however, the present study provides the first combined experimental and theoretical confirmation of such an assignment.

Conclusion

Reaction of $[M(N^tBu)_2(NH^tBu)_2]$, with various dianionic salen ligands affords bis-imido complexes $[M(N^tBu)_2L]$. These compounds adopt the strained β-*cis* configuration and this is apparently dictated by electronic rather than steric factors. The bis-imido Schiff base series $[M(N^tBu)_2L]$ display $[M(N^tBu)_2L]^{0/-1}$ redox couples confirmed by the EPR spectrum of chemically generated $\mathbf{1}^-$. The stability of these radical anions may be Schiff base dependent. The series of compounds **1**–**7** display unusually low energy one electron oxidation. The oxidation process is imido ligand centred as shown by the EPR spectrum of chemically and electrochemically generated $\mathbf{1}^+$. Density function calculations show that the HOMO is delocalised over both imido nitrogens. This arrangement may be an additional factor in stabilising the observed bis-imido *cis*-stereochemistry. It is clearly of interest to establish whether the delocalisation seen in the HOMO of complex **1** and $\mathbf{1}^+$ is a more general feature of *cis* bis-imido six-coordinate metal complexes and indeed other complexes with isolobal *cis*-π-base ligands.

Experimental

General details

Unless stated otherwise, all manipulations were generally carried out under an atmosphere of dry nitrogen using standard Schlenk/cannula techniques and a conventional nitrogen filled glove-box. Solvents were dried over the appropriate drying agent and distilled according to the literature procedure. Deuterated solvents were refluxed in *vacuo* over calcium hydride before trap-to trap distillation. All solvents were stored in reservoirs equipped with Young's taps over the appropriate activated molecular sieves, under a nitrogen atmosphere and degassed prior to use.

The NMR spectra were recorded on JEOL 270 (^{1}H, 270 MHz; ^{13}C{^{1}H}, 67.88 MHz), Bruker AMX400 (^{1}H, 400 MHz; ^{13}C{^{1}H}, 100.61 MHz) and AMX600 (^{1}H, 600 MHz; ^{13}C{^{1}H}, 150.90 MHz) spectrometers and referenced using residual protio-solvent resonance or tetramethylsilane at δ 0 ppm. Chemical shifts are quoted in δ (ppm) and coupling constants in Hertz. Assignments were supported by DEPT-135 and DEPT-90 homo- and heteronuclear, two-dimensional experiments as appropriate. EPR spectra were recorded on a Bruker 200D X-Band spectrometer. Infrared spectra were obtained using a Perkin Elmer FTIR 1720X spectrometer equipped with an ATR attachment, in the range 4000–400 cm^{-1}. Microanalyses were obtained from the service at Queen Mary. Mass spectra were obtained from the EPSRC Mass Spectroscopy Service, Swansea, Wales using LSIMS (liquid secondary ion mass spectrometry): caesium ion bombardment at 25 kV energy to the sample dissolved in a matrix liquid, typically 3-nitrobenzyl alcohol (NOBA), and polyethylene glycol (PEG) as a mass reference.

The compounds WCl_6, Na_2MoO_4, $AgPF_6$, 2,4-di-*tert*-butylphenol, *para*-formaldehyde, ethylenediamine, salicylaldehyde, 2-hydroxy-3-methoxybenzaldehyde, 2-hydroxy-4-methoxybenzaldehyde and 2-hydroxy-5-methoxybenzaldehyde were all purchased from Aldrich, Lancaster and Avocado chemical companies and used as received.

Literature methods were used for the preparation of $[W(N^tBu)_2(NH^tBu)_2]$,[13] $[Mo(N^tBu)_2Cl_2(dme)]$[14] $[Mo(N^tBu)_2(NH^tBu)_2]$[15] and the Schiff bases;[16] H_2salen, H_2(3-MeO)$_2$salen, H_2(4-MeO)$_2$salen, H_2(5-MeO)$_2$salen and H_2(3,5-^{t}Bu$_2$)$_2$salen.

Syntheses

3,5-Di-*tert*-butyl-2-hydroxybenzaldehyde. To a two-neck round bottom flask (2 L) equipped with a reflux condenser, magnetic stirrer and a nitrogen source was added anhydrous toluene (250 cm^3), 2,4-di-*tert*-butylphenol (100.0 g, 0.48 mol), tin(IV) tetrachloride (13 g, 5.86 cm^3, 0.05 mol) and tri-*n*-butylamine (37.0 g, 47.56 cm^3, 0.2 mol). The resulting yellow solution was stirred for 20 min at room temperature after which time *para*-formaldehyde (33.0 g, 1.1 mol) was added. The reaction mixture was then heated at ~100 °C for 16 h. After cooling, the reaction mixture was poured into distilled water (~2.5 L) acidified to pH 2 with 2 M HCl (~20 cm^3) and extracted with diethyl ether (~1 L). The ether extracts were washed with a saturated NaCl (500 cm^3) solution, the unreacted paraformaldehyde was filtered off, and the extracts were then dried ($MgSO_4$) and concentrated (rotary evaporator). The crude product was a mixture of 2,4-di-*tert*-butylphenol and 3,5-di-*tert*-butyl-2-hydroxybenzaldehyde, which was then recrystallised from methanol (500 cm^3) at 4 °C to leave 3,5-di-*tert*-butyl-2-hydroxybenzaldehyde (64.56 g, 57%); mp 59 °C.

^{1}H NMR ($CDCl_3$, 270 MHz 298 K): δ 11.56 (s, 1H, OH), 9.80 (s, 1H, CHO), 7.55 (s, 1H, arom. H), 7.29 (s, 1H, arom. H), 1.42 (s, 9H, ^{t}Bu), 1.32 (s, 9H, ^{t}Bu).

Preparation of $[W(N^tBu)_2\{(3,5\text{-}^tBu_2)_2salen\}]$ (1). To a solution of $[W(N^tBu)_2(NH^tBu)_2]$ (0.5 g, 1.06 mmol) in toluene (40 cm^3) was added solid H_2(3,5-^{t}Bu$_2$)$_2$salen (0.52 g, 1.06 mmol). The solution immediately turned orange and was then heated at reflux for 16 h. The orange reaction solution was then allowed to cool to room temperature, where it was dried under reduced pressure to produce analytically pure $[W(N^tBu)_2\{(3,5\text{-}^tBu_2)_2salen\}]$ (0.86 g, 99.3%). X-Ray quality crystals of $[W(N^tBu)_2\{(3,5\text{-}^tBu_2)_2salen\}]$ were grown from a concentrated toluene (10 cm^3) solution at −20 °C. mp 209–216 °C (with decomposition).

IR (cm^{-1}): 2958m, 2915m, 1640m, 1628m, 1599s, 1527m, 1461m, 1435s, 1386m, 1350m, 1267s, 1253s, 1239s, 1209br s, 1168s, 1133m, 1035m, 934m, 780s, 595s, 551s, 518s, 479s.

^{1}H NMR (d$_6$-benzene, 600 MHz, 298 K): δ 7.8 (d, $^4J_{H-H}$ = 2.8 Hz, 1H, aro H$_6$), 7.69 (d, $^4J_{H-H}$ = 2.8 Hz, 1H, arom. H$_6$), 7.5 (s, 1H, imine-H), 7.4 (s, 1H, imine-H), 7.16 (d, $^4J_{H-H}$ = 2.8 Hz, 1H, arom. H$_4$), 7.0 (d, $^4J_{H-H}$ = 2.8 Hz, 1H, arom. H$_4$), 3.84 (m, 1H, CH$_2$), 3.03 (m, 1H, CH$_2$), 2.98 (m, 1H, CH$_2$), 2.55 (m, 1H, CH$_2$), 1.50 (s, 9H, ^{t}Bu), 1.42 (s, 9H, ^{t}Bu), 1.13 (s, 9H, ^{t}Bu), 1.09 (s, 9H, ^{t}Bu), 0.95 (s, 9H, N^{t}Bu), 0.86 (s, 9H, N^{t}Bu).

^{1}H NMR ($CDCl_3$, 270 MHz 298 K): δ 8.16 (s, 1H, imine-H), 8.09 (s, 1H, imine-H), 7.52 (d, $^4J_{H-H}$ = 2.8 Hz, 1H, arom. H$_6$), 7.43 (d, $^4J_{H-H}$ = 2.8 Hz, 1H, arom. H$_6$), 7.08 (d, $^4J_{H-H}$ = 2.8 Hz, 1H, arom. H$_4$), 7.05 (d, $^4J_{H-H}$ = 2.8 Hz, 1H, arom. H$_4$), 4.45 (m, 1H, CH$_2$), 4.10 (m, 1H, CH$_2$), 3.95 (m, 1H, CH$_2$), 3.37 (m, 1H, CH$_2$), 1.46 (s, 9H, ^{t}Bu), 1.35 (s, 9H, ^{t}Bu), 1.33 (s, 9H, ^{t}Bu), 1.28 (s, 9H, ^{t}Bu), 1.03 (s, 9H, N^{t}Bu), 0.89 (s, 9H, N^{t}Bu).

^{13}C-{^{1}H} NMR (d$_6$-benzene, 150.90 MHz, 298 K): δ 170.61 (arom. C$_2$), 166.56 (C=N), 163.79 (arom. C$_2$), 162.69 (C=N), 141.92 (arom. C$_1$), 140.41 (arom. C$_1$), 138.91 (arom. C$_6$), 136.36 (arom. C$_6$), 130.52 (arom. C$_3$), 129.03 (arom. C$_3$), 128.55 (arom. C$_5$), 126.06 (arom. C$_5$), 124.62 (arom. C$_4$), 122.49 (arom. C$_4$), 66.67 (Me$_3$*C*N=), 66.30 (Me$_3$*C*N=), 65.71 (CH$_2$), 61.82 (CH$_2$), 36.16 (Me), 35.95 (Me), 34.15 (Me), 34.10 (Me), 32.80 (Me), 32.30 (Me), 31.91 (Me), 31.77 (Me), 31.64 (Me), 30.61 (Me), 30.47 (Me), 29.82 (Me), 29.49 (Me).

MS (LSIMS): *m*/*z* 817.4615 [M$^+$]; calc. for $C_{40}H_{64}N_4O_2W$: 817.4617 [M$^+$].

Preparation of $[W(N^tBu)_2\{(3\text{-}MeO)_2salen\}]$ (2). To a solution of $[W(N^tBu)_2(NH^tBu)_2]$ (0.5 g, 1.06 mmol) in toluene (40 cm^3) was added solid H_2(3-MeO)$_2$salen (0.35 g, 1.06 mmol). The solution immediately turned orange and was then heated at reflux for 16 h. The resulting brown reaction mixture was then allowed to cool to room temperature whereupon a yellow

precipitate, analytically pure [W(N^{t}Bu)$_2${(3-MeO)$_2$salen}] formed (0.54 g, yield = 74.6%), mp 186–188 °C (with decomposition).

IR (cm^{-1}): 2960w, 1642m, 1602s, 1581s, 1535m, 1468w, 1437m, 1415m, 1395m, 1328m, 1278s, 1239vs, 1166m, 1068m, 1048m, 1022m, 971w, 940m, 886w, 870s, 849m, 740s, 642w, 616m, 606m, 523m, 485m, 471m, 450m, 422m.

NMR: ^{1}H ($CDCl_3$, 270 MHz, 298 K): δ 8.25 (s, 1H, imine-H), 8.10 (s, 1H, imine-H), 7.1 (dd, 1H, arom. H_6), 6.95 (m, 3H, arom. H_4, H_4, H_6), 6.7 (t, $^3J_{H-H}$ = 7.93 Hz, 1H, arom. H_5), 6.5 (t, $^3J_{H-H}$ = 7.93 Hz, 1H, arom. H_5), 4.5 (m, 1H, CH_2), 4.2 (m, 1H, CH_2), 4.0 (m, 1H, CH_2), 3.96 (s, 3H, OMe), 3.94 (s, 3H, OMe), 3.5 (m, 1H, CH_2), 1.06 (s, 9H, N^{t}Bu), 0.94 (s, 9H, N^{t}Bu).

^{13}C-{^{1}H} ($CDCl_3$, 67.88 MHz, 298 K): δ 166.40 (arom. C_2), 162.83 (C=N), 162.15 (arom. C_2), 157.18 (C=N), 152.20 (arom. C_3), 150.85 (arom. C_3), 127.61 (arom. C_1), 126.80 (arom. C_1), 123.85 (arom. C_6), 123.80 (arom. C_6), 122.97 (arom. C_5), 122.69 (arom. C_5), 119.61 (arom. C_4), 103.52 (arom. C_4), 67.14 (CH_2), 66.03 (2× Me_3CN=), 62.01 (CH_2), 55.44 (OMe), 55.39 (OMe), 32.36 (Me), 31.95 (Me).

MS (LSIMS): *m*/*z* 653.2329 [M$^+$]; calc. for $C_{26}H_{36}N_4O_4W$: 653.2324 [M$^+$].

Preparation of [W(N^{t}Bu)$_2${(4-MeO)$_2$salen}] (3). To a solution of [W(N^{t}Bu)$_2$(NH^{t}Bu)$_2$] (0.5 g, 1.06 mmol) in toluene (40 cm^3) was added solid H_2(4-MeO)$_2$salen (0.35 g, 1.06 mmol). The solution immediately turned orange and was then heated at reflux for 16 h. After cooling to room temperature the solvent was removed under reduced pressure to produce analytically pure [W(N^{t}Bu)$_2${(4-MeO)$_2$salen}] (0.66 g, 95.7%), mp 196–198 °C (with decomposition).

IR (cm^{-1}): 2965w, 2953w, 2928w, 1635w, 1594 br s, 1542m, 1517m, 1435m, 1388m, 1273m, 1236s, 11.93s, 1206s, 1163s, 1116s, 1030s, 1935m, 1948m, 960m, 846m, 798m, 732m, 638s, 558m, 466m.

NMR: ^{1}H ($CDCl_3$, 270 MHz, 298 K): δ 8.13 (s, 1H, imine-H), 8.02 (s, 1H, imine-H), 7.13 (m, 2H, arom. H_6), 6.67 (d, $^4J_{H-H}$ = 2.21 Hz, 1H, arom. H_3), 6.47 (d, $^4J_{H-H}$ = 2.22 Hz, 1H, arom. H_3), 6.39 (dd, 1H, arom. H_5), 6.25 (dd, 1H, arom. H_5), 4.37 (m, 1H, CH_2), 4.16 (m, 1H, CH_2), 3.93 (m, 1H, CH_2), 3.83 (s, 3H, OMe), 3.77 (s, 3H, OMe), 3.46 (m, 1H, CH_2), 1.06 (s, 9H, N^{t}Bu), 1.01 (s, 9H, N^{t}Bu).

^{13}C-{^{1}H} ($CDCl_3$, 67.88 MHz, 298 K): δ 174.66 (arom. C_2), 168.13 (C=N), 166.73 (arom. C_2), 165.42 (C=N), 164.66 (arom. C_4), 161.40 (arom. C_4), 134.84 (arom. C_1), 132.92 (arom. C_1), 125.42 (arom. C_6), 116.90 (arom. C_6), 107.57 (arom. C_3), 106.95 (arom. C_3), 104.4 (arom. C_5), 103.52 (arom. C_5), 67.14 (CH_2), 66.03 (2 × Me_3CN=), 62.01 (CH_2), 55.44 (OMe), 55.39 (OMe), 32.36 (Me), 31.95 (Me).

MS (LSIMS): *m*/*z* 653.2320 [M$^+$]; calc. for $C_{26}H_{36}N_4O_4W$ 653.2324 [M$^+$].

Preparation of [W(N^{t}Bu)$_2${(5-MeO)$_2$salen}] (4). To a solution of [W(N^{t}Bu)$_2$(NH^{t}Bu)$_2$] (0.5 g, 1.06 mmol) in toluene (40 cm^3) was added solid H_2(5-MeO)$_2$salen (0.35 g, 1.06 mmol). The solution immediately turned orange and was then heated at reflux for 16 h. The brown reaction mixture was then allowed to cool to room temperature whereupon a yellow precipitate, analytically pure [W(N^{t}Bu)$_2${(5-MeO)$_2$salen}] formed (0.35 g, yield = 51%), mp 172–176 °C (with decomposition).

IR (cm^{-1}): 2969m, 2953m, 1645m, 1615s, 1593m, 1552w, 1528m, 1474m, 1442m, 1381w, 1322m, 1272s, 1240s, 1207br s, 1149m, 1124m, 1016m, 945m, 900m, 856m, 798m, 755s, 624m, 454m,

NMR: ^{1}H ($CDCl_3$, 400 MHz, 300 K): δ 8.48 (s, 1H, imine-H), 8.36 (s, 1H, imine-H), 7.35 (m, 3H, arom. H_6, H_6, H_3), 7.25 (d, $^3J_{H-H}$ = 9.23, arom. H_3), 7.02 (dd, 1H, arom. H_4), 6.98 (dd, 1H, arom. H_4), 4.73 (m, 1H, CH_2), 4.47 (m, 1H, CH_2), 4.27 (m, 1H, CH_2), 4.07 (s, 3H, OMe), 4.04 (s, 3H, OMe), 3.77 (m, 1H, CH_2), 1.33 (s, 9H, N^{t}Bu), 1.28 (s, 9H, N^{t}Bu),

^{13}C-{^{1}H} ($CDCl_3$, 100.61 MHz, 300 K): δ 167.08 (arom. C_2), 164.66 (C=N), 161.14 (C=N), 160.25 (arom. C_2), 150.16 (arom. C_5), 148.50 (arom. C_5), 125.41 (arom. C_6), 123.89 (arom. C_1), 123.32 (arom. C_6), 121.40 (arom. C_3), 121.09 (arom. C_1), 120.35 (arom. C_3), 114.96 (arom. C_4), 110.01 (arom. C_4), 65.92 (CH_2), 64.96 (2 × Me_3CN=), 61.10 (CH_2), 55.06 (OMe), 54.90 (OMe), 31.08 (Me), 30.74 (Me).

MS (LSIMS): *m*/*z* 653.2317 [M$^+$]; calc. for $C_{26}H_{36}N_4O_4W$: 653.2324 [M$^+$].

Preparation of [W(N^{t}Bu)$_2$(salen)] (5). To a solution of [W(N^{t}Bu)$_2$(NH^{t}Bu)$_2$] (0.5 g, 1.06 mmol) in toluene (40 cm^3) was added H_2salen (0.28 g, 1.06 mmol) as a solid. On addition an orange precipitate was formed. The reaction mixture was then heated at reflux for 16 h, darkening the solution. The produced dirty red/brown solution was then allowed to cool to room temperature, whereupon a fluffy yellow precipitate was produced, analytically pure [W(N^{t}Bu)$_2$(salen)]: 0.23 g, 36.5%), mp 151–154 °C (with decomposition).

IR (cm^{-1}): 2962w, 1646m, 1616m, 1605m, 1551w, 1527w, 1473m, 1442m, 1270m, 1240s, 1199m, 1146m, 1124m, 1015m, 944m, 899m, 854w, 797m, 755vs, 741m, 624s, 576m, 560m, 500m, 481m, 452m, 416m.

NMR: ^{1}H ($CDCl_3$, 270 MHz, 298 K): δ 8.27 (s, 1H, imine-H), 8.14 (s, 1H, imine-H), 7.38 (m, 4H, arom. *H$_5$, H$_5$, H$_6$, H$_6$*), 7.13 (dd, 1H, arom. H_3), 7.02 (dd, 1H, arom. H_3), 6.80 (dt, 1H, arom. H_4), 6.61 (dt, 1H, arom. H_4), 4.46 (m, 1H, CH_2), 4.23 (m, 1H, CH_2), 4.01 (m, 1H, CH_2), 3.53 (m, 1H, CH_2), 1.04 (s, 9H, N^{t}Bu), 0.96 (s, 9H, N^{t}Bu).

^{13}C-{^{1}H} ($CDCl_3$, 67.88 MHz, 298 K): δ 172.37 (arom. C_2), 166.82 (C=N), 166.60 (arom. C_2), 162.80 (C=N), 136.22 (arom. C_1), 134.12 (arom. C_1), 133.90 (arom. C_6), 131.48 (arom. C_6), 126.69 (arom. C_3), 123.49 (arom. C_3), 122.97 (arom. C_5), 121.95 (arom. C_5), 117.99 (arom. C_4), 115.59 (arom. C_4), 67.30 (Me_3CN=), 66.37 (CH_2), 66.27 (Me_3CN=), 62.41 (CH_2), 32.25 Me), 31.96 (Me).

MS (LSIMS): *m*/*z* 593.2122 [M$^+$]; calc. for $C_{24}H_{32}N_4O_2W$: 593.2113 [M$^+$].

Preparation of [Mo(N^{t}Bu)$_2${(3,5-^{t}Bu$_2$)$_2$salen}] (6). To a pale yellow solution of [Mo(N^{t}Bu)$_2$(NH^{t}Bu)$_2$] (0.50 g, 1.31 mmol) in toluene (~40 cm^3) was added solid H_2(3,5-^{t}Bu$_2$)$_2$salen (0.64 g, 1.31 mmol). The solution immediately turned orange and the reaction mixture was then refluxed for 16 h after which it was allowed to cool to room temperature. The volatiles were then removed under reduced pressure to leave an orange solid, analytically pure [Mo(N^{t}Bu)$_2${(3,5-^{t}Bu$_2$)$_2$salen}] (0.89 g, 94%). X-Ray quality crystals of [Mo(N^{t}Bu)$_2${(3,5-^{t}Bu$_2$)$_2$salen}] were grown from a concentrated toluene solution at −20 °C, mp 200–202 °C (with decomposition).

IR (cm^{-1}): 2959m, 2934w, 1640m, 1611m, 1601m, 1525w, 1434m, 1384w, 1351w, 1294w, 1254s, 1205 br s, 1165m, 1106m, 1022br s, 933m, 802s, 796s, 782s, 750m, 737m, 615m, 583m, 561m, 472m, 427s.

NMR: ^{1}H ($CDCl_3$, 270 MHz, 298 K): δ 8.24 (s, 1H, imine-H), 8.10 (s, 1H, imine-H), 7.46 (d, $^4J_{H-H}$ = 2.17 Hz, 1H, arom. H_6), 7.39 (d, $^4J_{H-H}$ = 2.17 Hz 1H, arom. H_6), 7.07 (d, $^4J_{H-H}$ = 2.17 Hz, 1H, arom. H_4), 7.02 (d, $^4J_{H-H}$ = 2.17 Hz, 1H, arom. H_4), 4.25 (m, 1H, CH_2), 3.9 (m, 2H, CH_2), 3.35 (m, 1H, CH_2), 1.44 (s, 9H, ^{t}Bu), 1.37 (s, 9H, ^{t}Bu), 1.33 (s, 9H, ^{t}Bu), 1.28 (s, 9H, ^{t}Bu), 1.07 (s, 9H, N^{t}Bu), 0.94 (s, 9H, N^{t}Bu).

^{13}C-{^{1}H} ($CDCl_3$, 67.88 MHz, 298 K): δ 170.47 (arom. C_2), 165.42 (C=N), 165.09 (arom. C_2), 162.56 (C=N), 141.43 (arom. C_1), 139.58 (arom. C_1), 137.81 (arom. C_6), 135.27 (arom. C_6), 129.88 (arom. C_3), 128.43 (arom. C_3), 128.37 (arom. C_5), 124.64 (arom. C_5), 124.13 (arom. C_4), 121.62 (arom. C_4), 69.57 (Me_3CN=), 69.15 (Me_3CN=), 64.80 (CH_2), 62.08 (CH_2), 35.96 (Me), 35.71 (Me), 34.21 (Me), 34.08 (Me), 31.79 (Me), 31.52 (Me), 30.98 (Me), 30.18 (Me), 30.05 (Me).

MS (LSIMS): *m/z* 731.4160 [M^+]; calc. for $C_{40}H_{64}N_4O_2Mo$: 731.4162 [M^+].

Preparation of [Mo(N^{t}Bu)$_2${(4-MeO)$_2$salen}] (7). To a pale yellow solution of [Mo(N^{t}Bu)$_2$(NH^{t}Bu)$_2$] (0.50 g, 1.31 mmol) in toluene (~ 40 cm^3) was added H_2(4-MeO)$_2$salen (0.43 g, 1.31 mmol). The solution immediately turned orange and was then heated at reflux for 16 h. The dark orange reaction solution was then allowed to cool to room temperature and solvents and volatiles removed under reduced pressure to produce analytically pure [Mo(N^{t}Bu)$_2${(4-MeO)$_2$salen}] (0.71 g, 96%), mp 209–219 °C (with decomposition).

IR (cm^{-1}): 2962w, 1625w sh, 1601br m, 1523 w, 1515m, 1438m, 1387w, 1352w, 1291w, 1258m, 1214s, 1205s, 1165m, 1115m, 1024s, 1024br s, 971m, 830m, 751s, 774s, 659m, 638m, 604m, 459m.

NMR: ^{1}H (d_6-benzene, 270 MHz, 298 K): δ 7.53 (s, 1H, imine-H), 7.40 (s, 1H, imine-H), 7.06 (m, 3H, arom. H_6, H_6, H_3), 6.71 (d, $^4J_{H-H}$ = 2.24 Hz, 1H, arom. H_3), 6.53 (m, 2H, arom. H_5, H_5), 3.8 (m, 2H, CH_2), 3.23 (s, 3H, OMe), 3.19 (s, 3H, OMe), 3.10 (m, 1H, CH_2), 2.8 (m, 1H, CH_2), 1.29 (s, 9H, N^{t}Bu), 1.20 (s, 9H, N^{t}Bu).

^{13}C-{^{1}H} ($CDCl_3$, 67.88 MHz, 298 K): δ 174.56 (arom. C_2), 169.24 (C=N), 166.07 (arom. C_2), 164.41 (C=N), 164.10 (arom. C_4), 161.30 (arom. C_4), 134.82 (arom. C_1), 132.64 (arom. C_1), 125.22 (arom. C_6), 116.31 (arom. C_6), 106.63 (arom. C_3), 106.07 (arom. C_3), 103.85 (arom. C_5), 103.46 (arom. C_5), 70.02 (Me_3CN=), 69.22 (Me_3CN=), 64.82 (CH_2), 61.55 (CH_2), 55.17 (OMe), 55.13 (OMe), 30.64 (Me), 30.54 (Me).

MS (LSIMS): *m/z* 566.1777 [M^+]; calc. for $C_{26}H_{36}N_4O_4Mo$: 566.1791 [M^+].

Preparation of [Mo(N^{t}Bu)$_2$(salen)] (8). To a pale yellow solution of [Mo(N^{t}Bu)$_2$(NH^{t}Bu)$_2$] (0.50 g, 1.31 mmol) in toluene (40 cm^3) was added H_2salen (0.35 g, 1.31 mmol). This reaction mixture was heated at reflux for 16 h, at ~100 °C when all the H_2salen dissolved into the orange toluene solution. Then the now dirty brown reaction solution was allowed to cool to room temperature, producing a yellow precipitate, [Mo(N^{t}Bu)$_2$-(salen)] (0.3 g, 45%), mp 147–151 °C (with decomposition).

IR (cm^{-1}): 2960w, 2950w, 1655w, 1617s, 1592s, 1548m, 1481m, 1443s, 1342w, 1330w, 1292br s, 1242m, 1218s, 1206s, 1148m, 1123m, 1111m, 1014m, 939m, 900brm, 850m, 753w, 741w, 624m, 612m, 457m, 452m.

NMR: ^{1}H ($CDCl_3$, 270 MHz, 298 K): δ 8.34 (s, 1H, imine-H), 8.20 (s, 1H, imine-H), 7.27 (m, 4H, arom. H_5, H_5, H_6, H_6), 7.06 (m, 2H, arom. H_3), 6.76 (t, $^3J_{H-H}$ = 7.93 Hz, 1H, arom. H_4), 6.56 (t, $^3J_{H-H}$ = 7.93 Hz, 1H, arom. H_4), 4.2 (m, 1H, CH_2), 3.95 (m, 2H, CH_2), 3.5 (m, 1H, CH_2), 1.07 (s, 9H, N^{t}Bu), 1.00 (s, 9H, N^{t}Bu).

^{13}C-{^{1}H} ($CDCl_3$, 67.88 MHz, 298 K): δ 172.4 (arom. C_2), 168.1 (C=N), 166.0 (arom. C_2), 162.9 (C=N), 135.9 (arom. C_1), 135.2 (arom. C_1), 134.3 (arom. C_6), 131.6 (arom. C_6), 125.3 (arom. C_3), 123.7 (arom. C_3), 122.6 (arom. C_5), 121.5 (arom. C_5), 117.8 (arom. C_4), 115.6 (arom. C_4), 71.4 (Me_3CN=), 69.8 (Me_3CN=), 65.2 (CH_2), 61.9 (CH_2), 31.1 (Me).

MS (LSIMS): *m/z* 506.1595 [M^+]; calc. for $C_{24}H_{32}N_4O_2Mo$: 506.1579 [M^+].

X-Ray crystallography

Data were collected at 120 K using a Nonius Kappa CCD area detector diffractometer mounted at the window of molybdenum rotating anode (50 kV, 90 mA, λ = 0.71069 Å). The crystal-to-detector distance was 45 mm and ϕ and Ω scans (0.7° increments, 84 s exposure time) were carried out to fill the Ewald sphere. Data collection and processing were carried out using the COLLECT,[17] DENZO[18] and maXus[19] and empirical absorption correction was applied using SORTAV.[20] The structure was solved by the heavy-atom method using DIRDIF99[21] and refined anisotropically (non-hydrogen atoms) by full-matrix least-squares on F^2 using the SHELXL-97[22] program. The H atoms were calculated geometrically and refined with riding model. The program ORTEP-3[23] was used for drawing the molecule. WINGX[24] was used to prepare material for publication.

Crystal data for **1**: $C_{40}H_{66}MoN_4O_2$, M = 730.91, triclinic, space group $P\bar{1}$, a = 10.7723(3), b = 14.2968(3), c = 14.0076(4) Å, α = 65.273(1), β = 84.677(1), γ = 81.976(1)°, V = 1939.90(9) Å^3, Z = 2, D_c = 1.252 Mg m^{-3}, μ = 0.376 mm^{-1}, reflections measured 29831, reflections unique 9363 with R_{int} = 0.0735, T = 150(2) K, Final R indices {$I > 2\sigma(I)$}; $R1$ = 0.0466, $wR2$ = 0.1209 and for all data $R1$ = 0.0607, $wR2$ = 0.1277.

CCDC reference number 209224.

See http://www.rsc.org/suppdata/dt/b3/b304627c/ for crystallographic data in CIF or other electronic format.

Electrochemical studies

Cyclic voltammetry experiments were performed using a VersaStat EG&G Princeton Applied Research potentiostat and an EG&G VersaStat II Princeton Applied Research potentiostat with Model 270/250 Research Electrochemistry Software v 4.00.

The electrochemical cell used for the cyclic voltammetry experiments was an undivided glass cell equipped with three electrodes. The working electrode was a platinum disk ($\varnothing$ = 0.5–1 mm) sealed into glass. The reference electrode was a simple silver wire in a glass tube with a porous glass tip. The counter electrode was a platinum wire in a glass tube with a porous glass tip. The cell was sealed under nitrogen before and during the experiment. This electrode was calibrated using the reversible reduction potential of cobaltocenium hexafluorophosphate as standard after each measurement. A 0.1 M ^{n}Bu$_4$NPF$_6$ was used as a supporting electrolyte in all cases. Sample concentration was typically 10^{-3} M.

Controlled electrolysis

Compound **1** (0.3 g, 0.37 mmol) in 0.2 M ^{n}Bu$_4$NPF$_6$ in DMF (25 cm^3) was added to the anodic compartment of a two compartment cell divided by a glass filter (electrolyte solution in the cathodic compartment) a Pt electrode in each compartment. The required Faradaic charge was passed through the cell at 100 mA constant current at room temperature. Compound **1**$^+$ was transferred to a quartz cell for EPR measurements.

EPR (298 K): quintet g_{av} = 2.015, a = 10.93 G.

Chemical oxidation

In a 250 cm^3 round bottom flask covered in aluminium foil was placed $AgPF_6$ (0.11 g, 0.44 mmol) in THF (30 cm^3) in the dark. To this solution was added an orange solution of [W(N^{t}Bu)$_2$-{(3,5-^{t}Bu$_2$)$_2$salen}] (0.36 g, 0.44 mmol) in THF in the dark. On addition a dark precipitate was deposited from the yellow solution. This reaction mixture was then syringed into a foil covered EPR tube equipped with a Young's tap adapter and examined by EPR spectroscopy in the temperature range 140–310 K. EPR (298 K): quintet g_{av} = 2.015, a = 10.93 G.

Chemical reduction

Freshly cut sodium metal portions (0.17 g, 7.39 mmol) were carefully dropped into mercury (20 cm^3). To this freshly prepared sodium mercury amalgam was slowly dropped a solution of [W(N^{t}Bu)$_2${(3,5-^{t}Bu$_2$)$_2$salen}] (6.00 g, 7.35 mmol) in THF (40 cm^3), with stirring. This orange reaction mixture was then left to stir for 2 h to produce a dark brown solution. An aliquot of this reaction mixture was then syringed into an EPR tube equipped with a Young's tap adapter and examined by EPR spectroscopy.

EPR (298 K): singlet g_{av} = 1.998.

Density function calculations

The calculations were conducted without symmetry constraints using the Amsterdam Density Functional program, version 2000.01.[25–29] The basis sets employed were valence-only, uncontracted Slater type orbitals of dz1p quality on the main group elements and hydrogen (ADF Type III), while for tungsten triple-zeta valence functions were used (ADF Type IV). The frozen core approximation was employed (W.4d, C.1s, N.1s, O.1s), scalar relativistic corrections[27] were included *via* the ZORA to the Dirac equation,[30–32] and the local density parameterisation of Vosko, Wilk and Nusair was used.[33]

Acknowledgements

We thank EPSRC for a Quota award to R. R.; Peter Haycock and Dr Harold Toms from University of London Interdisciplinary Research Service for NMR; Professor J. Utley (QM) for use of cyclic voltammetry equipment; EPSRC National Mass Spectrometry Service for mass spectra and the EPSRC National Crystallography Service for data collection.

References

1 (*a*) M. P. Coles, C. I. Dalby, V. C. Gibson, W. Clegg and M. R. J. Elsegood, *J. Chem. Soc., Chem. Commun.*, 1995, 1709; M. P. Coles, C. I. Dalby, V. C. Gibson, W. Clegg and M. R. J. Elsegood, *Polyhedron*, 1995, **14**, 2455; M. P. Coles, V. C. Gibson, W. Clegg, M. R. J. Elsegood and P. Porrelli, *Chem. Commun.*, 1996, 1963; (*b*) R. L. Zuckerman and R. G. Bergman, *Organometallics*, 2001, **20**, 1792; J. W. Bruno and X. J. Li, *Organometallics*, 2000, **19**, 4672; R. L. Zuckerman, S. W. Krska and R. G. Bergman, *J. Am. Chem. Soc.*, 2000, **122**, 751; W. D. Wang and J. H. Espenson, *Organometallics*, 1999, **18**, 5170; J. M. McInnes, A. J. Blake and P. Mountford, *J. Chem. Soc., Dalton Trans.*, 1998, 3623; G. K. Cantrell and T. Y. Meyer, *J. Am. Chem. Soc.*, 1998, **120**, 8035.
2 M. Motevalli, B. C Parkin, R. Ramnauth and A. C. Sullivan, *J. Chem. Soc., Dalton Trans.*, 2000, 2661.
3 D. E. Wigley, *Prog. Inorg. Chem.*, 1994, **42**, 239; W. A. Nugent and B. L. Haymore, *Coord. Chem. Rev.*, 1980, **31**, 123.
4 J. M. McInnes, D. Swallow, A. J. Blake and P. Mountford, *Inorg. Chem.*, 1998, **37**, 5970.
5 P. R. Woodman, I. J. Munslow, P. B. Hitchcock and P. Scott, *J. Chem. Soc., Dalton Trans.*, 1999, 4069.
6 M. C. W. Chan, F.-W. Lee, K.-K. Cheung and C.-M. Che, *J. Chem. Soc., Dalton Trans.*, 1999, 3197.
7 W.-H. Leung, M.-C. Wu, T.-C. Lau and W.-T. Wong, *Inorg. Chem.*, 1995, **34**, 4271.
8 K. Srinivasan and J. K. Kochi, *Inorg. Chem.*, 1985, **24**, 4671.
9 W.-H. Leung, M.-C. Wu, K.-Y. Wong and Y. Wang, *J. Chem. Soc., Dalton Trans.*, 1994, 1659.
10 M. H. Schofield, T. P. Kee, J. T. Anhaus, R. R. Schrock, K. H. Johnson and W. M. Davis, *Inorg. Chem.*, 1991, **30**, 3595.
11 S.-M. Lee, R. Kowallick, M. Marcaccio, J. A. McCleverty and M. D. Ward, *J. Chem. Soc., Dalton, Trans.*, 1998, 3443.
12 A. A. Danopoulos, G. Wilkinson, T. K. N. Sweet and M. B. Hursthouse, *J. Chem. Soc., Dalton Trans.*, 1995, 937.
13 W. A. Nugent and R. L. Harlow, *Inorg. Chem.*, 1977, **19**, 777.
14 P. W. Dyer, V. C. Gibson, J. A. K. Howard, B. Whittle and C. Wilson, *J. Chem. Soc., Chem. Commun.*, 1992, 1666.
15 A. A. Danopoulos, G. Wilkinson, B. Hussain-Bates and M. B. Hursthouse, *J. Chem. Soc., Dalton Trans.*, 1990, 2753.
16 M. Calligaris and L. Randaccio, in *Comprehensive Coordination Chemistry*, ed. G. Wilkinson, R. D. Gillard, and J. A. McCleverty, Pergamon, Oxford, 1987, vol. 2, p. 715.
17 R. Hooft, Collect, Data Collection Software, Nonius B. V., Delft, The Netherlands, 1998.
18 Z. Otwinowski and W. Minor, *Methods Enzymol.*, 1997, **276**, 307–326.
19 S. Macay, C. J. Gilmore, C. Edwards, M. Tremayne, N. Stuart and K. Shankland, maXus, Computer Program for the Solution and Refinement of Crystal Structure from Diffration data, University of Glasgow, Nonius B. V., Delft and MacScience Co. Ltd., Yokohama, 1998.
20 (*a*) R. H. Blessing, *Acta Crystallogr., Sect A*, 1995, **51**, 33–37; (*b*) R. H. Blessing, *J. Appl. Crystallogr.*, 1997, **30**, 421–426.
21 P. T. Beurskens, G. Beurskens, W. P. Bosman, R. de Gelder, S. Garcia-Granda, R. O. Gould, R. Israel and J. M. M. Smits, DIRDIF99 program system, Crystallography Laboratory, University of Nijmegen, The Netherlands, 1999.
22 G. M. Sheldrick, SHELXL-97, Program for Refinement of Crystal Structures, University of Göttingen, Germany, 1997.
23 L. J. Farrugia, *J. Appl. Crystallogr.*, 1997, **30**, 565.
24 L. J. Farrugia, *J. Appl. Crystallogr.*, 1999, **32**, 837–838.
25 ADF2000, Department of Theoretical Chemistry, Vrije Universiteit, Amsterdam, 2000.
26 E. J. Baerends, D. E. Ellis and P. Ros, *Chem. Phys.*, 1973, **2**, 41.
27 L. Versluis and T. Ziegler, *J. Chem. Phys.*, 1988, **88**, 322.
28 G. te Velde and E. J. Baerends, *J. Comput. Phys.*, 1992, **99**, 84.
29 C. Fonseca Guerra, J. G. Snijders, G. te Velde and E. J Baerends, *Theor. Chem. Acc.*, 1998, **99**, 391.
30 N. Kaltsoyannis, *J. Chem. Soc., Dalton Trans.*, 1997, 1.
31 E. van Lenthe, R. van Leeuwen, E. J. Baerends and J. G. Snijders, *Int. J. Quantum Chem.*, 1996, **57**, 281.
32 E. van Lenthe, J. G. Snijders and E. J. Baerends, *J. Chem. Phys.*, 1996, **105**, 6505.
33 S. H. Vosko, L. Wilk and M. Nusair, *Can. J. Phys.*, 1980, **58**, 1200.